Title	A new indirect anisotropic quadrilateral mesh generation scheme with enhanced local mesh smoothing procedures
Author(s)	Lee, Y. K.; Lee, Chi King
Citation	Lee, Y. K.,& Lee, C. K. (2003). A new indirect anisotropic quadrilateral mesh generation scheme with enhanced local mesh smoothing procedures. International Journal for Numerical Methods in Engineering, 58(2), 277-300.
Date	2003
URL	http://hdl.handle.net/10220/19234
Rights	© 2003 John Wiley & Sons Ltd. This is the author created version of a work that has been peer reviewed and accepted for publication by International Journal for Numerical Methods in Engineering, John Wiley & Sons Ltd. It incorporates referee's comments but changes resulting from the publishing process, such as copyediting, structural formatting, may not be reflected in this document. The published version is available at: [Article DOI: http://dx.doi.org/10.1002/nme.771].

A New Indirect Anisotropic Quadrilateral Mesh Generation Scheme with Enhanced Local Mesh Smoothing Procedures

Y. K. Lee[1] and *C. K. Lee[2]

School of Civil and Environmental Engineering
Nanyang Technological University
Nanyang Avenue
Singapore 639798

*E-mail address: ccklee@ntu.edu.sg

Pre-printed version of the paper appeared in the journal:
International Journal for Numerical Methods in Engineering, Vol 58, No. 2, pp277-300

Summary

An enhanced version of indirect advancing front technique is proposed for the construction of full quadrilateral anisotropic meshes on 3D surfaces. The final quadrilateral mesh is constructed from a background triangular mesh and the merging procedure is carried out in the parametric space. The proposed method employed the systemic merging technique for the formation of quadrilaterals and the metric specifications for controlling the anisotropic characteristics of the elements. In order to generate well graded anisotropic quadrilaterals, the selection criteria of base segment for merging are carefully defined. Furthermore, in order to improve the shape quality of the final mesh, a set of new local smoothing algorithms for anisotropic quadrilateral mesh quality enhancement has been proposed and tested in this study. Numerical examples obtained indicate that the proposed enhanced local smoothing schemes can effectively improve the quality of the quadrilateral meshes produced and increase the robustness of the mesh generation scheme.

KEYWORDS: *Anisotropic mesh generation; Advancing front technique; Indirect quadrilateral mesh generation; Systemic merging technique; Local and global anisotropic mesh smoothings*

---

[1] Research Fellow, current address: Fluent INC 500 Davis Street, Suite 600, Evanston, IL 60201, USA
[2] Associate Professor

1 Introduction

Recently, the topic of unstructured surface anisotropic quadrilateral mesh generation has received much attention since a full surface quadrilateral mesh is the prerequisite for complete unstructured hexahedral mesh generation. Furthermore, because of the better efficiency and accuracy of quadrilateral elements over triangular elements, there is a constant demand to develop a robust quadrilateral mesh generator for 3D surface meshing and many different generation algorithms have been suggested [1-12]. Towards this end, all existing unstructured quadrilateral meshing algorithms can be grouped into two main categories, namely, the *direct* and the *indirect* approaches.

In the direct algorithms, quadrilateral elements are directly constructed over the problem domains. Using bi-sectioning and pre-designed templates, Talbert and Parkinson [1] proposed an algorithm to generate quadrilateral meshes in 2D domains. Zhu et al. [2] proposed an *advancing front technique* (AFT) for forming and merging two triangular elements at a time. Blacker [3] developed the well-known *paving algorithm* for 2D quadrilateral meshing. The paving algorithm was extended to 3D surfaces by Cass et al. [4] and then later by White and Kinney [5] for enhancing the stability of the element formation procedure.

In the indirect algorithms, quadrilaterals are formed by converting two or more triangular elements at a time in an existing *background triangular mesh* that can be created by using any triangular mesh generator. Lo [6] first suggested an algorithm which converts a triangular mesh into a mixed mesh with dominant number of quadrilateral elements. Johnston et al. [7] then developed additional procedures such as local splitting and swapping to further increase the proportion of quadrilateral elements. Rank et al. [8] proposed a technique to transform triangular meshes into quadrilateral meshes by splitting two neighbouring triangles. Lee et al. [9,10] later extended their work to generate full quadrilateral meshes by introducing the *systemic merging technique* (SMT). By combining the SMT with techniques used in the paving algorithm, Owen et al [11] developed the *Q-MORPH* algorithm for planar and surface quadrilateral mesh generations. Recently, Lee and Lee [12] further extended Owen et al.'s work and successfully developed a conversion algorithm for the generation of anisotropic quadrilateral meshes over general curved surfaces. In their work, it was found that the criteria for the selection of *base front segment* for the quadrilateral formation step will greatly affect the quality of the final mesh created.

Besides the base segment selection criteria, it was reported [2,9-12] that the quality of the final quadrilateral mesh can be improved by applying some carefully designed *structural modifications* and *mesh smoothing procedures* either locally during the conversion phase or globally as *ad doc* mesh quality enhancement procedures after the conversion phase is completed.

Mesh smoothing is a technique frequently employed by many researchers to improve the quality of meshes by repositioning nodes without altering the connectivity of the elements. Hermann [13] proposed a unified weighed smoothing approach for 2D meshes to improve the shape quality of elements by progressively moving a node to the centroid of its surrounding polygon. Beside the standard weighed smoothing approach, other smoothing techniques based on the geometrical properties of the elements were also proposed [14,15]. In some approaches, global or local measures quantifying elements quality are employed, and the new positions of nodes are obtained by optimising the functional derived from the distortion measure used [16-18]. Blacker [3] proposed a set of heuristic local smoothing algorithms and Owen et al. [11] suggested a set of local mesh smoothing techniques for indirect quadrilateral mesh generation. Lee [19,20] proposed the edge length smoothing and element quality smoothing techniques to improve the quality of anisotropic meshes. Hyun and Lindgren [21] examined the effects of different mesh smoothing schemes on graded elements during an adaptive finite element analysis. In addition, a special smoothing algorithm for the optimisation for a quadrilateral mesh with invalid elements was proposed and tested by Li et al. [22]. Note that most of the above smoothing techniques can either be applied locally during the meshing procedure or globally after the mesh generation procedure is completed.

The main objective of this study is to present a new indirect quadrilateral mesh generation scheme over 3D curved surfaces. The proposed method is an improved extension of the anisotropic quadrilateral mesh generation scheme proposed recently by Lee and Lee [12]. In this study, a new set of heuristic local smoothing procedures specially designed for the use in the general anisotropic case, has been implemented and tested. This set of newly developed smoothing algorithms is designed to improve the local quality of the mixed mesh along the merging front during the incremental conversion procedure. Numerical testing indicates that the new smoothing algorithms are able to further improve the quality of the final anisotropic quadrilateral meshes.

2 Overview of the conversion procedure and elementary mesh modification operations

2.1 Overview of the conversion procedure

The present method is an indirect method with the basic principle that a full quadrilateral mesh can be formed by carefully converting two or more triangles at a time in the background triangular mesh to form one new quadrilateral element (Fig. 1). By repeating such operations, quadrilateral elements can be constructed to cover the whole problem domain provide that the number of segments enclosing the background triangular mesh is even. The geometry of the target surface is represented by a bi-variate mapping approach and metric specifications are employed for the control of element size and the anisotropic characteristics of the mesh. Detailed descriptions of the geometrical model used and the metric specifications can be found in references [20,23-25] and a brief summary is given in Appendix A for completeness. The whole conversion scheme can be divided into the following essential steps:

(i) Background triangular mesh generation
(ii) Formation of initial front
(iii) Base segment selection for quadrilateral formation
(iv) Edge recovery for quadrilateral element formation and merging front update
(v) Local post-processing (local structural modifications and local smoothings)
(vi) Global post-processing

The detailed operations for steps (i) to (iv) and step (vi) for the current conversion scheme are essentially the same as the previous version suggested in reference [12], and hence, only brief summaries of them will be given in Section 3. For step (v), the local structural modifications procedures used are again very similar to those used in reference [12]. However, a new set of enhanced local smoothing schemes has been implemented and tested in this study to improve the shape quality and grading of the quadrilateral mesh produced. More details of the enhanced smoothing schemes developed will be given in Section 3.

2.2 Elementary mesh modification operations

Elementary mesh modifications are operations that are frequently used during the conversion and the local post-processing. Five such operations are used and a concise summary of them is given below.

(1) Edge swapping

In edge swapping, the edge shared by two elements is replaced by a new edge linking the opposite nodes (Fig. 2) provide that the sum of the two angles of each end of the original edge should be less than 180°.

(2) Edge collapsing (element deletion)

In this operation, an edge shared by two elements will be removed and the two elements adjacent to the edge will be deleted (Fig. 3).

(3) Edge division

During edge division, an edge will be divided at its midpoint and the two adjacent elements will be divided into four elements (Fig. 4).

(4) Node deletion

Two types of node deletion processes are implemented in this study. In the three-element case, the node completely surrounded by three elements will be removed (Fig. 5a). In the four-element case, after the node is deleted a new edge spanning the shorter diagonal will be created (Fig. 5b).

(5) Edge recovery procedure

When an edge connecting a pair of nodes is needed, the assumed edge is recovered by the edge recovery procedure [26]. As demonstrated in Fig. 6, the assumed edge is recovered by carrying out a series of edge swapping operations on the elements that intersect the assumed edge.

3 Implementation of the quadrilateral conversion algorithm

3.1 Generation of background triangular mesh

As the proposed scheme is designed to generate unstructured anisotropic quadrilateral meshes, the element size distribution of the input background triangular mesh should be compatible with the user metric specifications, $\mathbf{M_{3D}}$ (Eqn. A2). In this study, the surface anisotropic mesh triangulator developed by Lee [20] is used, and the surface metric tensor, **M** (Eqn. A3), will be defined at all the nodal points of the background mesh.

3.2 Formation of initial merging front

At the beginning of the conversion process, the merging front is taken as the boundary of the background mesh, and the following information will be received from the background mesh.

(1) The length, l, of the front segments (Eqn. A4).

(2) Elements (and hence nodes and edges) that are connected to the front segments.

(3) The left and right neighbour segments of the front segments.

(d) The internal frontal angle θ_A (Eqn. A5) of the front segments (Fig. 7a).

3.3 Base segment selection

The base segment will determine both the *location* of the new element and the *advancing direction* of the merging front. No single criterion will always yield optimal results under all different element size requirements. An extensive study carried out previously [12] showed that for the general anisotropic case, good base front segments can be selected by considering the *H-values* of the front segments. For the segment AB shown in Fig. 7a, its H-value, H_{AB}, is defined as

$$H_{AB} = \frac{1}{2}\left(\frac{1}{\sqrt{\max\left(\lambda_1^A, \lambda_2^A\right)}} + \frac{1}{\sqrt{\max\left(\lambda_1^B, \lambda_2^B\right)}} \right) \tag{1}$$

In Eqn. 1, λ_i^A and λ_i^B i=1,2 are the eigenvalues of the metric tensors for nodes A and B respectively. During base segment selection, both H_{AB} and the frontal angles θ_A and θ_B (Fig. 7a) will be considered, and preference will be given to segments with small values of H_{AB} and frontal angles closed to an ideal value θ_{rect}. In the current study, an additional option for the selecting the base segment using the level criterion is also implemented. For the details of the selection procedure, one may refer to reference [12].

3.4 Edges preparation and quadrilateral formation

After the base segment is selected, a new quadrilateral will be created by the following steps.

(i) Prepare the left and right side edges of the new quadrilateral (Fig. 7b).

(ii) Recover the top edge connecting the two top nodes of the side edges (Fig. 7c).

(iii) Merge all the triangular elements enclosed by the four side edges into a quadrilateral (Fig. 7d).

In general, the three additional edges (left, right and top) do not always exist and they are obtained or created by using a series of elementary operations (Section 2.2) [12]. The two side edges are selected from the edges connected to the two end nodes A and B of the base segment. In order to obtain a well shaped quadrilateral consistent with the user specification, both the lengths of the edges and their angles with the base segment

will be considered. In addition, if needed, the selected side edge will be divided or swapped in order to maintain the even segment condition of the generation front [12].

After the left and right side edges are defined, the edge linking the two top nodes of the two side edges is the last edge to be prepared. If such an edge does not exist, it has to be recovered by an edge recovery procedure similar to the one mentioned in Section 2.2. However, sometime it is necessary to carry out other elementary operations to recover the top edge (Fig. 8). In fact, in some exceptional situations, it is required to re-construct the right side edge or even both side edges before the top edge can be recovered [11,12].

After all the four side edges are prepared, a new quadrilateral element is created by eliminating all the triangular elements bounded by the side edges and it can be shown easily that the total number of front segments will always remain even.

3.5 Local mesh post-processing

During the quadrilateral formation step, the element connectivity of the local mesh surrounding the base segment is frequently altered by the elementary mesh modification operations, highly distorted elements may be formed and the quality of the local mesh surrounding the newly formed quadrilateral element may be deteriorated. If these distorted elements are left untreated, the robustness of subsequent quadrilateral formation steps may be affected. As a result, after a new quadrilateral is formed, both local structural enhancements and local mesh smoothing will be carried out to improve the quality and validity of the local mesh.

3.5.1 Local structural enhancements

In the local structural enhancements, the connectivity of the local mesh will be modified to restore the validity of the local mesh surrounding the newly formed quadrilateral. Three types of local structural enhancement procedures are implemented.

(1) Structural enhancement by elementary operations [12]

In this procedure, all edges and elements around the new quadrilateral are examined. The node deletions and swapping procedures will be carried out to eliminate elements with very big or very small internal angles as shown in Fig. 9.

(2) Frontal segment seaming

This procedure is employed when the frontal angle between two adjacent front segments is less than or equal to 30°. As shown in Fig. 10, if there is no edge linking the two end nodes B and C, such an edge will be recovered by a procedure

similar to the one used for top edge recovery during the quadrilateral formation step (Fig. 10b). The seaming operation will then be completed by collapsing this edge (Fig. 10c). In case that the lengths of two edges to be seamed could be very different, the transition seam techniques proposed by Blacker [3] and Owen et al. [11] could be employed to obtain more optimal result.

(3) Merging front splitting [12]

In some cases after a new quadrilateral is formed, the merging front may enclose a very narrow region, and the merging front splitting operation is employed to prevent the formation of an excessively slender elements. As shown in Fig. 11, the slender element will be deleted, and the merging front will be modified accordingly.

3.5.2 Local mesh smoothing

The main function of local mesh smoothing is to reposition the nodes surrounding the newly formed quadrilateral so that the shape qualities of both the newly formed quadrilateral and its neighbouring elements will be improved. In the current work, a study was carried out to investigate the effects of different local smoothing schemes on the shape quality of the final mesh produced. Similar to the case of base segment selection, it was found that no single local smoothing scheme can yield optimal results under different combinations of element connectivity and grading requirements. After some careful studies and from the previous works by Blacker [3] and Owen et al. [11], during the repositioning of a given node in the local mesh, different smoothing schemes should be used according to the number of its adjacent quadrilateral elements. In order to restore a well graded anisotropic local mesh after a new quadrilateral is formed, three specially designed local smoothing schemes are proposed and implemented in the present work. It should be pointed out that while the basic ideas of these smoothing schemes were adopted from the works of Lee [19,20], Blacker [3] and Owen et al. [11], major extensions are made to modify and implement them to work optimally in the general anisotropic case.

(1) Floating node smoothing

A *floating node* is a node on the newly formed quadrilateral which connects to only one quadrilateral element. As shown in Fig. 12, if $N_I N_J N_K N_L$ is the newly formed quadrilateral element, node N_I is the floating node of the quadrilateral. Numerical experimentation indicates that when repositioning N_I, the best result is obtained by

considering the shape quality of the quadrilateral $N_IN_JN_KN_L$. (Note that node N_I also connects to other unconverted triangular elements.) During the floating node smoothing, the adjustment of the node is decomposed into two directions: along the direction of the vectors $\overrightarrow{N_JN_I}$ and $\overrightarrow{N_LN_I}$ as shown Fig. 12a. Since the ideal distance between nodes N_I and N_J should equal to unity (in the normalized metric space), Δ_{IJ}^{D}, the length adjustment in parametric coordinates of node N_I in the $\overrightarrow{N_JN_I}$ direction can be computed as

$$\Delta_{IJ}^{D} = \left(1 - \frac{1}{\tilde{l}(N_I, N_J)}\right)\begin{Bmatrix} u_I - u_J \\ v_I - v_J \end{Bmatrix} \tag{2}$$

In Eqn. 2, (u_I,v_I) and (u_J,v_J) are the parametric coordinates of nodes N_I and N_J respectively and $\tilde{l}(N_I,N_J)$ is the metric length of the edge N_IN_J. The above length adjustment will alter the angle between the edges N_LN_I and N_KN_L. Hence, in order to reflect the effect of such angular change, another adjustment term, Δ_{IJ}^{A}, the angular adjustment of N_I in the $\overrightarrow{N_JN_I}$ direction is computed by taking the arc length into account as shown in Fig. 12b.

$$\Delta_{IJ}^{A} = \theta \cdot \tilde{l}(N_I, N_L)\frac{\overrightarrow{N_IN_J}}{\left\|\overrightarrow{N_IN_J}\right\|} \tag{3}$$

In Eqn. 3, θ is the deviation of the angle $\angle N_IN_LN_K$ from 90°.

The adjustment of N_I in the $\overrightarrow{N_JN_I}$ direction, Δ_{IJ}, is then computed as the linear combination of Δ_{IJ}^{D} and Δ_{IJ}^{A} and is given by

$$\Delta_{IJ} = \omega\Delta_{IJ}^{D} + (1-\omega)\Delta_{IJ}^{A} \tag{4a}$$

In Eqn. 4a, the weight factor $0 \le \omega \le 1$ is taken as 0.5 in this study. Similarly, Δ_{IL}, the adjustment in the $\overrightarrow{N_LN_I}$ direction can be expressed as

$$\Delta_{IL} = \omega\Delta_{IL}^{D} + (1-\omega)\Delta_{IL}^{A} \tag{4b}$$

where Δ_{IL}^{D} and Δ_{IL}^{A} are respectively the length and angular adjustments in the $\overrightarrow{N_LN_I}$ direction, and they can be obtained by applying Eqns. 2 and 3 to nodes N_I and N_L.

The final adjustment of node N_I is taken as the sum of the adjustments in both directions.

$$\Delta = \Delta_{IJ} + \Delta_{IL} \tag{5}$$

An iterative procedure of the above algorithm is implemented, and an example for a simple configuration of a quadrilateral element is given in Fig. 13 to demonstrate the convergence of the smoothing procedure. From Fig. 13, it can be seen that the floating node settled at the ideal position within a few iterations.

(2) Row node smoothing

The row node smoothing method is applicable to nodes which are adjacent to only two quadrilateral elements sharing a common edge. The basic idea of this smoothing method was first proposed by Blacker in the paving algorithm [3] and it is now extended to the general anisotropic case in this study.

In the smoothing of the row nodes, the adjustment is also decomposed into two parts, the length adjustment, Δ_l, and the angular adjustment, Δ_C, as shown in Fig. 14. The length adjustment is determined by the following procedure.

(i) Compute the initial length adjustment, Δ_i, of node N_I using an anisotropic version of the standard isoparametric smoothing scheme [13]

$$\Delta_i = \hat{\mathbf{P}}_{\mathrm{I}} - \mathbf{P}_{\mathrm{I}}, \quad \hat{\mathbf{P}}_{\mathrm{I}} = \frac{1}{\mathrm{NP}} \sum_{\alpha=1}^{\mathrm{NP}} \left(\mathbf{P}_{\mathrm{J}}^{\alpha} + \mathbf{P}_{\mathrm{L}}^{\alpha} - \mathbf{P}_{\mathrm{K}}^{\alpha} \right) \tag{6a}$$

In Eqn. 6, $\mathbf{P}_{\beta}^{\alpha}$, where β=I,J,K,L and α=1,2 are the positions of nodes N_β (measured with respect to node N_J). NP=2 is the number of quadrilateral elements adjacent to node N_I, and $\hat{\mathbf{P}}_{\mathrm{I}}$ is the adjusted position of N_I.

(ii) Computation of Δ_l uses the following equation

$$\Delta_l = \overrightarrow{N_I N_J} + \left(\Delta_i - \overrightarrow{N_I N_J} \right) \frac{1}{\tilde{l}_i} \tag{6b}$$

The angular adjustment is employed to improve the orthogonality of the shared edge N_IN_J with the base segment. Since in this study the metric specifications are employed for element size control (Appendix A), any angular adjustment must take into the account the effect of the local metric specifications at N_I. Thus, before carrying out the angular adjustment, all the vectors involved such as $\mathbf{P}_{\mathrm{I}}$ and $\mathbf{P}_{\mathrm{B1}}$ must first be transformed by the following equation [19,23]

$$\mathbf{P}' = \mathbf{M}^{\frac{1}{2}}\mathbf{P} \tag{7}$$

In Eqn. 7, **M** is the metric tensor at node N_I. **P** and **P'** are the vectors before and after transformation respectively. By using the Eqn. 7, the angular adjustment of the node N_I can be computed by the following steps (Fig. 14b).

(i) Compute the vector $\mathbf{P}'_{\mathrm{B1}}$ which bisects the angle between the vectors $\mathbf{P}'_{\mathrm{I-1}}$ and $\mathbf{P}'_{\mathrm{I+1}}$.

(ii) Compute the vector $\mathbf{P}'_{\mathrm{B2}}$ which bisects the angle between the vector $\mathbf{P}'_{\mathrm{I}}$ and $\mathbf{P}'_{\mathrm{B1}}$.

(iii) Compute the point **Q** by intersecting $\mathbf{P}'_{\mathrm{B2}}$ with $\overrightarrow{N_{i-1}N_{i+1}} = \mathbf{P}'_{\mathrm{I+1}} - \mathbf{P}'_{\mathrm{I-1}}$.

(iv) Adjust the length of $\mathbf{P}'_{\mathrm{B2}}$ so that

$$\left\|\mathbf{P}'_{\mathrm{B2}}\right\| = \begin{cases} \left(\tilde{l}_{\mathrm{Q}} + 1\right)/2 & \text{if } \tilde{l}_{\mathrm{Q}} < 1 \\ 1 & \text{otherwise} \end{cases} \tag{8a}$$

where $\tilde{l}_{\mathbf{Q}}$ is the metric length of the vector $\overrightarrow{N_J\mathbf{Q}}$.

(v) Inverse transform $\mathbf{P}'_{\mathrm{B2}}$ and compute the angular adjustment, Δ_C as

$$\mathbf{P}_{\mathrm{B2}} = \mathbf{M}^{-\frac{1}{2}}\mathbf{P}'_{\mathrm{B2}} \tag{8b}$$

$$\Delta_C = \mathbf{P}_{\mathrm{B2}} - \mathbf{P}_{\mathrm{I}} \tag{8c}$$

The final total movement of N_I is then determined by averaging the two adjustments computed by Eqns. 6b and 8c such that

$$\Delta = \Delta_I + \Delta_C \tag{9}$$

In Fig. 15a, a simple configuration of two elements is used as an example to demonstrate the row node smoothing scheme. As one can expect, the ideal position of the row node should make the two quadrilateral elements become rectangles. Nodal positions obtained during successive smoothing iterations are shown in Fig. 15b. Note that because of the nature of the angular adjustment which tends to move the shared edge towards the bisecting line, the convergence rate of the nodal position decreases as the number of iterations increases. In practice, it is found that three iterations of the above row node smoothing procedure will be sufficient in most cases to improve the quality of the local mesh.

(3) Area-weighted smoothing

An anisotropic version [12] of the area-weighted smoothing algorithm suggested by Jones [14] is applied to all those nodes which are adjacent to either no or more than two quadrilateral elements. In this smoothing scheme, the new position of a node, $\mathbf{P}'$, will be computed as the weighed-centroid of its surrounding elements defined by

$$\mathbf{P}' = \frac{\sum_{i=1}^{NP} A_i \mathbf{C}_i}{\sum_{i=1}^{NP} A_i} \tag{10}$$

In Eqn. 10, NP is the number of elements (including both quadrilaterals and triangles) adjacent to the node. $\mathbf{C}_i$ is the centroid of the i-th element, E_i, surrounding the node under consideration, and A_i is the area of E_i.

(4) Order of local smoothing

From the numerical experiments done during the development of the above local smoothing algorithms, it was found that the order of application of the local smoothing schemes will also affect the quality of the final mesh produced. In this study, nodes of the local mesh surrounding the newly generated quadrilateral will be smoothed in the following order:

(i) Smooth the nodes on the newly generated quadrilateral element in the order of floating node, row node and other nodes.

(ii) Adjust the positions of other floating nodes connected to the newly generated quadrilateral.

(iii) Adjust the positions of other row nodes connected to the newly generated quadrilateral.

(iv) Adjust the positions of other neighbouring nodes that connect to the newly generated quadrilateral using the area-weighted smoothing scheme.

In the current implementation, steps (i) to (iv) will be repeated three times to obtain optimal result. In most cases, the above smoothing sequence will able to improve the local quality of neighbouring elements. However, for some exceptional cases, the floating node or the row node smoothing schemes may create elements with reverse orientation (negative area). This is due to the fact that these two smoothing schemes are carried out without considering the conditions of the surrounding triangles. Thus, in

order to make sure that all the elements produced are valid, during any local smoothing procedure after the new position of a node is computed, the areas of all its adjacent elements will be recalculated. In case at least one of them has negative area, the original positions of the local nodes will be recovered, and re-smoothing will be applied using the area-weighted smoothing algorithm.

3.6 Global Post Processing

By repeating the merging operation, the background triangular mesh will be converted into a full quadrilateral mesh. After the full quadrilateral mesh is formed, a set of standard mesh enhancement procedures [2,19,20] and mesh smoothing procedures will be applied to further enhance the quality of the output mesh.

4 Mesh generation examples

In this section, a few mesh generation examples will be presented to demonstrate the robustness and the performance of the proposed mesh generator.

4.1 Example one: Square plate with metric intersection

In the first example, a simple 2D anisotropic case is used to demonstrate the overall process of anisotropic SMT. The domain under consideration is a square plate. The metric tensor, $\mathbf{M}_1$, used was defined by the principal directions and characteristic distances shown in Fig. 16a and Eqn. 11.

$$\begin{aligned} h_1 &= 0.2 - 0.195\, e^{-d1} \\ h_2 &= 0.2 - 0.195\, e^{-d2} \end{aligned} \tag{11}$$

As shown in Fig. 16b, highly stretched elements along the two diagonal lines were generated for the background triangular mesh (779 nodes and 1460 elements). Figs. 16c to 16f show the intermediate and the final meshes (791 quadrilaterals) produced during the conversion procedure. From these figures, it can be seen that the merging front propagated towards the internal region along the lines of slender elements because the H-value decreased along that direction. For the same background mesh, another slightly different quadrilateral mesh was also formed by activating the level option for base segment selection so that a boundary layer of quadrilaterals was generated first. The intermediate and final meshes produced are shown in Fig. 17a and 17b respectively. As shown in Fig. 17a, a layer of elements was formed automatically along the external

boundary of the square before the merging front propagated into the interior of the problem domain.

4.2 Example two: Meshing for a wing

In the second example, the domain under consideration is an airplane wing with fictitious metric specifications. The original mesh was generated with 3341 nodes and 6360 triangles and it was converted to a quadrilateral mesh with 3336 nodes and 3176 quadrilaterals as shown in Fig. 18. From Fig. 18, one can see that both the anisotropic and the isotropic characteristics of the mesh were well preserved in the quadrilateral mesh. Thus, besides the general anisotropic case, it can be concluded that the developed method is also applicable to the isotropic case too.

4.3 Example three: Meshing for a nozzle

In this example, a 3D surface for a nozzle which consists of three sub-surfaces was employed to demonstrate the use of the proposed algorithm for 3D surfaces mesh generation. Fig. 19a and 19b show the geometry of the surface patch and metric specifications for mesh generation. The target characteristic length and metric tensor employed to generate the background triangular mesh (684 nodes and 1254 triangles, Fig. 19c) are given by

$$h_1 = 7.5 - 7.3e^{-0.05d}$$
$$h_2 = h_3 = \begin{cases} h & if \quad h = 75 - 73e^{-0.05d} < 10 \\ 10 & ,otherwise \end{cases} \tag{12}$$

The conversion was carried out in a surface by surface manner and the final quadrilateral mesh generated is shown in Fig. 19d. The anisotropic properties of the background mesh is preserved.

4.4 Example four: Mesh generation for cylindrical surface for speed and shape quality evaluations

In this example, the target surface is a quarter of cylindrical shell surface as shown in Fig. 20. In order to evaluate the performance of the proposed mesh conversion algorithm, a series of quadrilateral meshes with different element size density were generated by varying the parameter c given in Fig. 20. The background anisotropic triangular meshes were generated in such a way that the numbers of elements

approximately doubled as the value of c was reduced. Fig. 21 shows the background and the quadrilateral mesh produced for c=0.70, 0.55, 0.35 and 0.18. The mesh generator has been implemented using the Microsoft Visual C++ compiler with speed optimisation. The CPU times for conversion and mesh quality enhancement spent on a PC equipped with an Intel PIII 500MHz processor were logged and are listed in Table 1 and plotted in Fig 22 against the number of quadrilaterals generated, NQ. As shown in Fig. 22, the order of complexity of the present mesh conversion scheme is $O(NQ^{1.1})$. From Table 1, it can be seen that the actual speed of conversion is quite fast, and a mesh with 10,000 quadrilateral elements can be generated by using a low-end PC within 20 seconds. For the grading and shape quality of the meshes generated, the edge lengths and internal angles of elements (with respect to the metric specification) for the meshes with c=0.7 and 0.18 are plotted in Fig. 23. From Fig. 23a, it can been seen that when c=0.7 and the element size is large when comparing with the problem domain size, a bigger scattering in the edge length distribution was observed. However, as element sizes were decreased by setting c=0.18, most of the edge lengths converged to the ideal value of unity with considerably smaller scattering. Similar result can also be seen for the internal angles distribution of elements as shown in Fig. 23b. The difference between the minimum and the maximum internal angles is obviously reduced in the case of c=0.18 when compared with c=0.70.

5 Conclusions

A new indirect technique has been introduced to convert general anisotropic triangular meshes to full quadrilateral meshes. The proposed scheme is an enhanced extension of the anisotropic systemic merging technique developed previously by the authors. An extensive study was carried out to investigate the effect of different local smoothing schemes on the quality and grading of the quadrilateral mesh produced. By using an enhanced quadrilateral element formation scheme and a series of carefully designed local structural modification and local smoothing operations, the new mesh conversion procedure is robust for the formation of strongly anisotropic quadrilateral meshes. Furthermore, the anisotropic characteristics of the original meshes are well preserved in the final meshes. Numerical examples given indicated that in the quadrilateral meshes generated, most of the edges have normalized edge lengths close to the prefect value of unity and with internal angles within the optimal range.

Regarding the speed of the conversion, near linear time increase is achieved by localizing most operations during the quadrilateral element formation and the local post-processing steps. Detailed timings of the examples given show that the operational complexity of the conversion scheme is of order $O(NQ^{1.1})$ where NQ is the number of quadrilaterals generated. The overall speed of the present scheme is fast enough for most practical applications. By using a low-ended PC equipped with an Intel Pentium III 500MHz CPU, the present implementation can convert a highly graded anisotropic triangular mesh with about 20,000 elements into a full quadrilateral mesh with roughly 10,000 quadrilateral elements within 20 seconds.

Appendix A: Geometrical model and metric specifications

A1 Geometrical model used

In the present study, the problem domain under consideration will be represented as a union of surface patches and bi-variate non-uniform rational B-Spine (NURBS) surfaces of the form [20]

$$(x, y, z)^T = \mathbf{r}(u, v) \tag{A1}$$

will be used to define individual support surface. Furthermore, trimming curves, repeated lines, crack lines and surface branching will all be defined as NURBS curves in the parametric spaces of the support surfaces. This geometrical model is highly flexible and able to model most commonly encountered geometrical features in engineering applications.

A2 Metric Specifications

In the 3D space, the metric tensor is a symmetric positive definite matrix, $\mathbf{M}_{3D}$, such that $\mathrm{Det}(\mathbf{M}_{3D})>0$ and the eigenpairs of $\mathbf{M}_{3D}$, $(\mathbf{g}_i,\lambda_i)$, i=1,2,3, will represent the desired principal stretching directions and node spacing in the mesh [20,23]. If $\mathbf{d\xi}$ and $\mathbf{dx}$ are the elementary vectors in the normalized and the 3D spaces respectively, the length scale transformation is defined by

$$\mathbf{d\xi}^T\mathbf{d\xi} = \mathbf{dx}^T\mathbf{M}_{3D}\mathbf{dx} \tag{A2}$$

Using Eqn. A2, the 2×2 surface metric tensor, $\mathbf{M}$, that combines the effects of the user specifications of node space, $\mathbf{M}_{3D}$, and the surface mapping (Eqn. A1) can be defined as

$$\mathbf{M} = \begin{pmatrix} \dfrac{\partial \mathbf{r}}{\partial \mathrm{u}} & \dfrac{\partial \mathbf{r}}{\partial \mathrm{v}} \end{pmatrix}^{\mathsf{T}} \mathbf{M}_{3\mathrm{D}} \begin{pmatrix} \dfrac{\partial \mathbf{r}}{\partial \mathrm{u}} & \dfrac{\partial \mathbf{r}}{\partial \mathrm{v}} \end{pmatrix} \tag{A3}$$

For two points $\mathbf{p}_1(u_1,v_1)$ and $\mathbf{p}_2(u_1,v_2)$ in the parametric space, the distance between them with respect to $\mathbf{M}$, $l(\mathbf{M},\mathbf{p}_1\mathbf{p}_2)$, is defined as

$$l(\mathbf{M},\mathbf{p}_1\mathbf{p}_2) = \sqrt{\begin{pmatrix} u_2 - u_1 \\ v_2 - v_1 \end{pmatrix}^{\mathsf{T}} \mathbf{M} \begin{pmatrix} u_2 - u_1 \\ v_2 - v_1 \end{pmatrix}} \tag{A4}$$

The angle between two infinitesimal vectors **du** and **dv** with respect to **M**, $\theta(\mathbf{M},\mathbf{du},\mathbf{dv})$, is defined as

$$\theta(\mathbf{M},\mathbf{du},\mathbf{dv}) = \begin{cases} \cos^{-1}\left(\dfrac{(\mathbf{du})^{\mathsf{T}} \mathbf{M} \mathbf{dv}}{l(\mathbf{M},\mathbf{du}) \cdot l(\mathbf{M},\mathbf{dv})} \right) & \text{if } \mathbf{du} \times \mathbf{dv} > 0 \\ 2\pi - \cos^{-1}\left(\dfrac{(\mathbf{du})^{\mathsf{T}} \mathbf{M} \mathbf{dv}}{l(\mathbf{M},\mathbf{du}) \cdot l(\mathbf{M},\mathbf{dv})} \right) & \text{otherwise} \end{cases} \tag{A5}$$

It should be stressed that since in this study, the proposed mesh conversion scheme is designed to generate full quadrilateral anisotropic meshes for 3D surfaces, ***all*** the length and angle measurements carried out during the mesh conversion process will be referred to the normalized space using Eqns A4 and A5.

References

1. J. A. Talbert, J. A. and A. R. Parkinson, 'Development of an automatic two dimensional finite element mesh generator using quadrilateral elements and Bezier curve boundary definition', *Int. J. Numer. Meth. Engrg.,* **29**, 1551-1567 (1991)

2. J. Z. Zhu; O. C. Zienkiewicz, E. Hinton, J Wu, 'A new approach to the development of automatic quadrilateral mesh generation', *Int. J. Numer. Meth. Engrg.,* **32,** 849-866 (1991)

3. T. D. Blacker and M. B. Stephenson, 'Paving: A new approach to automated quadrilateral mesh generation', *Int. J. Numer. Meth. Engrg.,* **32,** 811-847 (1991)

4. R. J. Cass, S. E. Benzley, R. J. Meyers, T. D. Blacker, 'Generalized 3-D paving: An automated quadrilateral surface mesh generation algorithm', *Int. J. Numer. Meth. Engrg.,* **39,** 1475-1489 (1996)

5. D. R. White and P. Kinney, 'Redesign of the Paving algorithm: Robustness enhancements through element by element meshing', *Proc. 6th Int. Meshing Roundtable,* 323-335 (1997)

6. S. H. Lo, 'A new mesh generation scheme for arbitrary planar domain', *Int. J. Numer. Meth. Engrg.,* **21,** 1403-1426 (1985)

7. B. P. Johnston, J. M. Sullivan Jr., A. Kwasnik, 'Automatic conversion of triangular finite element meshes to quadrilateral elements', *Int. J. Numer. Meth. Engrg.,* **31,** 67-84 (1991)

8. E. Rank, M. Schweingruber, M. Sommer, 'Adaptive mesh generation and transformation of triangular to quadrilateral meshes', *Commun. Numer. Meth. Engrg.,* **9,** 121-129 (1993)

9. C. K. Lee and S. H. Lo, 'A new scheme for the generation of a graded quadrilateral mesh', *Comput. Struct.,* **52,** 847-857 (1994)

10. T. S. Lau, S. H. Lo, C. K. Lee, 'Generation of quadrilateral mesh over analytical curved surface', *Fin. Elem. Ana. Design,* **27,** 251-272 (1997)

11. S. J. Owen, M. L. Staten, S. A. Canann, S. Saigal, 'Q-MORPH: An indirect approach to advancing front quad meshing', *Int. J. Numer. Meth. Engrg.,* **44,** 1317-1340 (1999)

12. Y. K. Lee and C. K. Lee, 'Automatic generation of anisotropic quadrilateral meshes on three dimensional surfaces using metric specifications', *Int. J. Numer. Meth. Engrg.,* accepted for publication.

13. L. R. Hermann, 'Laplacian-isoparametric grid generation scheme', *J. Engrg. Mech. Div. ASCE,* **102,** EM5, 749-756 (1976)

14. R. E. Jones, 'A self-organizing mesh generation program', *J. Pressure Vessel Tech. Trans. ASME,* **96(3)**, 193-199 (1974)

15. J. U. Brackbill and J. S. Saltzman, 'Adaptive smoothing for singular problems in two dimensions', *J. Computational Physics,* **46,** 342-368 (1982)

16. S. A. Canann, M. B. Stephenson, T. Blacker, 'Optismoothing: An optimization-driven approach to mesh smoothing', *Fin. Elem. Ana. Design,* **13,** 185-190 (1993)

17. A. Oddy, J. Goldak, J. M. McDill, J. M. Biddy, 'A distortion metric for iso-parametric finite elements', *Tran. Can. Soc. Mech. Engrg.,* **12(4),** 213-217 (1988)

18. P. J. Frey and H. Borouchaki, 'Surface mesh quality evaluation', *Int. J. Numer. Methods. Engrg.,* **45,** 101-118 (1999)
19. C. K. Lee, 'Automatic adaptive mesh generation using metric advancing front approach', *Engrg. Computations,* **16,** 230-263 (1999)

20. C. K. Lee, 'Automatic metric advancing front triangulation over curved surfaces', *Engrg. Computations,* **17,** 48-74 (2000)

21. S. Hyun and L. Lindgren, 'Smoothing and adaptive remeshing schemes for graded element', *Commun. Numer. Methods. Engrg.,* **17,** 1-17 (2001)

22. T. S. Li, S. M. Wong, Y. C. Hon, C. G. Armstrong, R. M. McKeag, 'Smoothing by optimisation for a quadrilateral with invalid elements', *Fin. Elem. Ana. Design,* **34,** 37-60 (2000)

23. H. Borouchaki, P. L. George, F. Hecht, P. Laug, S. Saltl, 'Delaunay mesh generation governed by metric specifications. Part I. Algorithms', *Fin. Elem. Ana. Design,* **25,** 61-83 (1997)

24. H. Borouchaki, P. L. George, F. Hecht, P. Laug, E. Saltl, 'Delaunay mesh generation governed by metric specifications. Part II. Applications', *Fin. Elem. Ana. Design,* **25,** 85-109 (1997),

25. H. Borouchaki, P. J. Frey, 'Adaptive triangular-quadrilateral mesh generation', *Int. J. Numer. Meth. Engrg., 41,* 915-934 (1998)

26. P. L. George, F. Hecht, E. Saltel, 'Automatic mesh generator with specified boundary', *Comput. Meth. Appl. Mech. Engrg.,* **92,** 269-288 (1991)

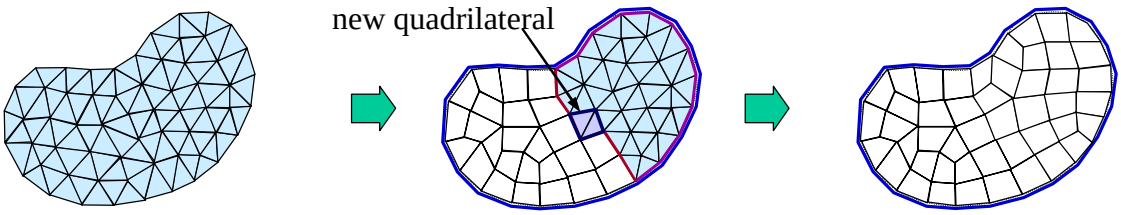

Background triangular mesh

Intermediate configuration after some quadrilateral elements are formed

Final full quadrilateral mesh

Figure 1. Basic mesh conversion principle.

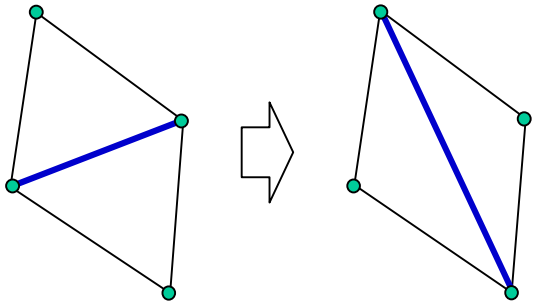

(a)

Figure 2. Edge swapping.

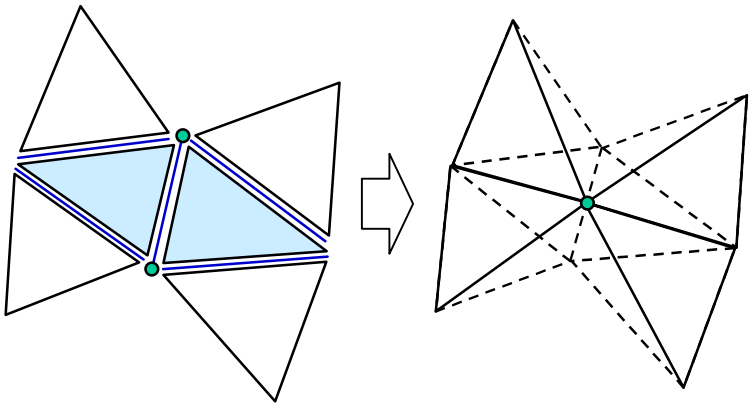

Figure 3. Edge collapsing (element deletion) operation.

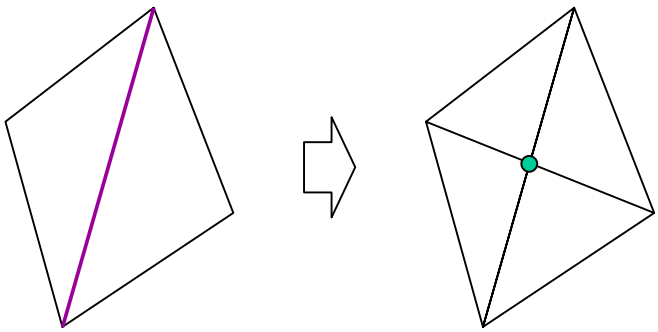

Figure 4. Edge division operation.

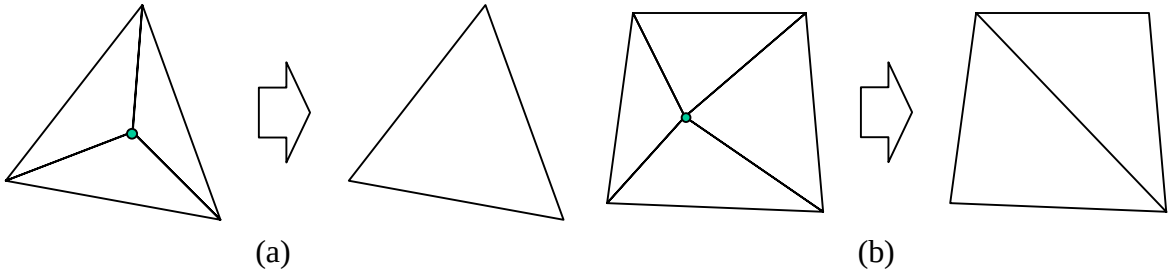

Figure 5. Node deletion: (a) three-element case; (b) four-element case.

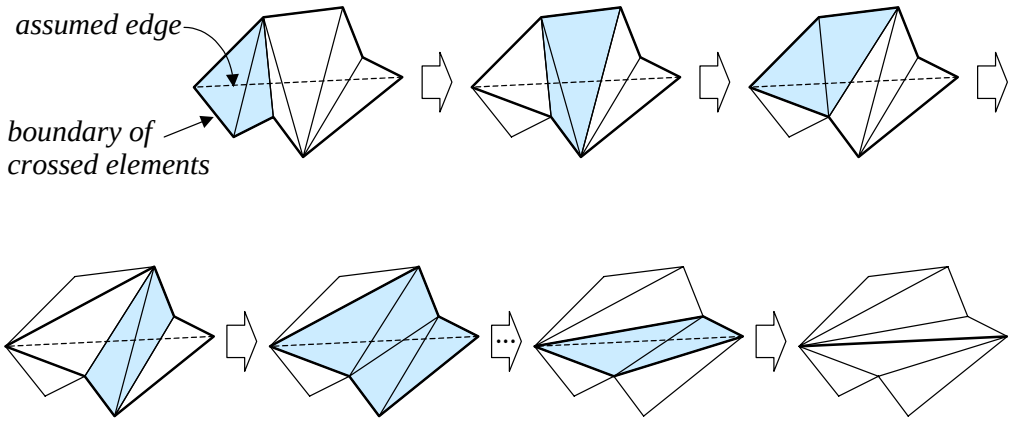

Figure 6. Edge recovery.

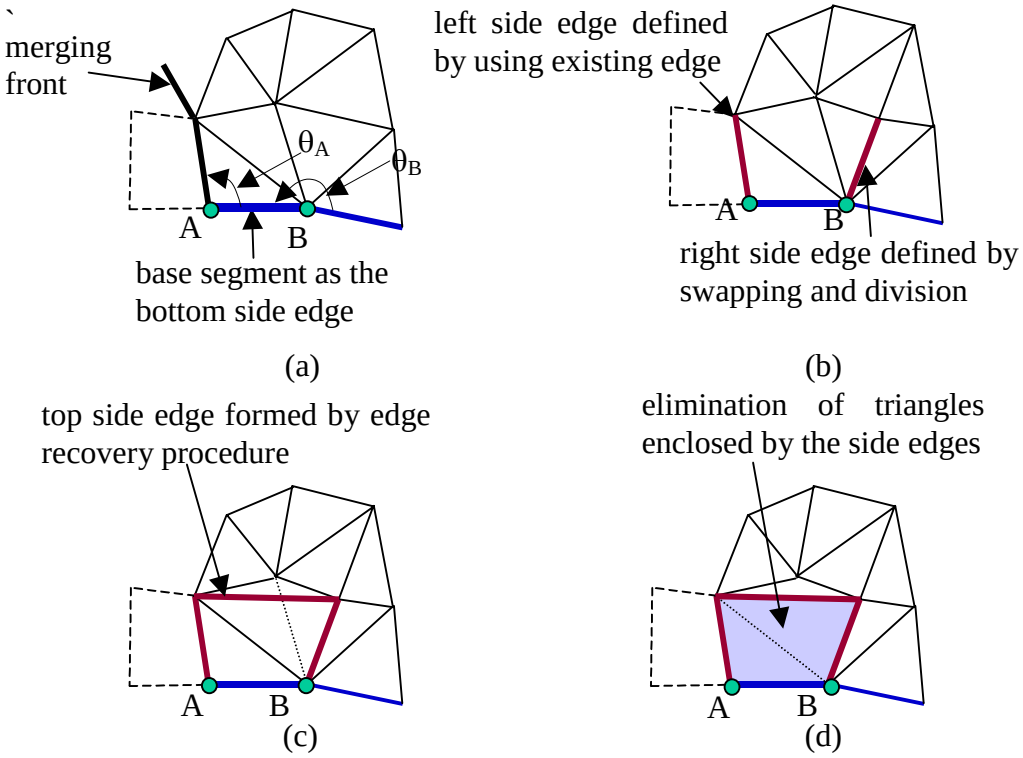

Figure 7. Formation of quadrilateral element: (a) base segment as bottom side edge; (b) preparation of left and right side edges; (c) recovery of top side edge; (d) merging for quadrilateral formation.

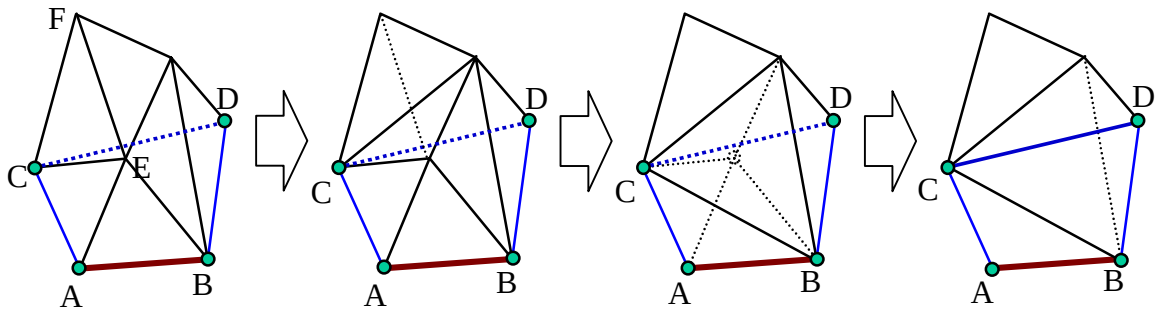

Figure 8. Top edge recovery procedure.

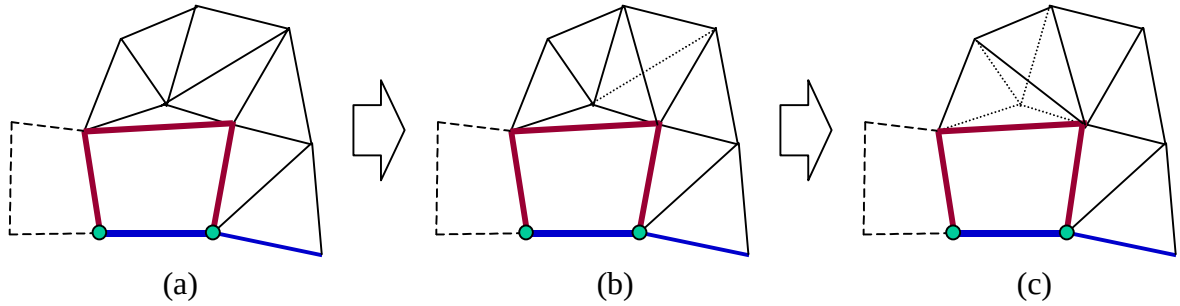

Figure 9. Local structural enhancement using elementary operations: (a) original local mesh; (b) swapping of edge; (c) node deletion.

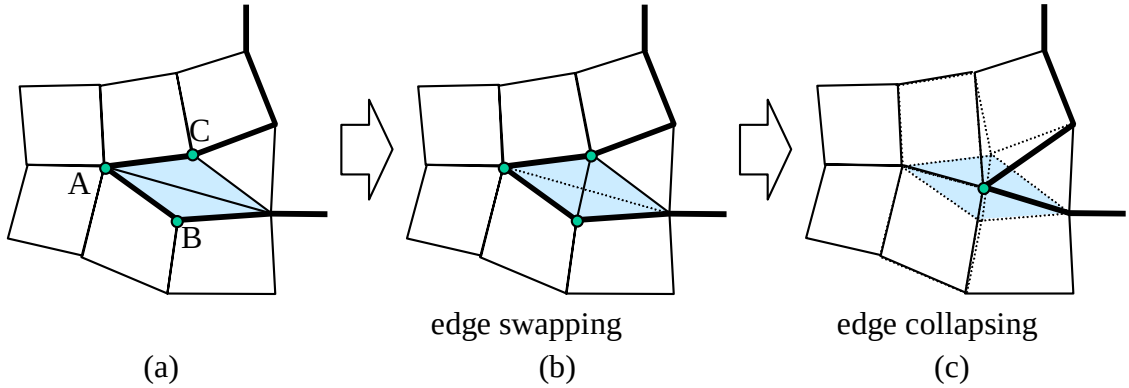

Figure 10. Frontal segment seaming: (a) adjacent segment with small frontal angle; (b) edge recovery operation; (c) edge collapsing operation.

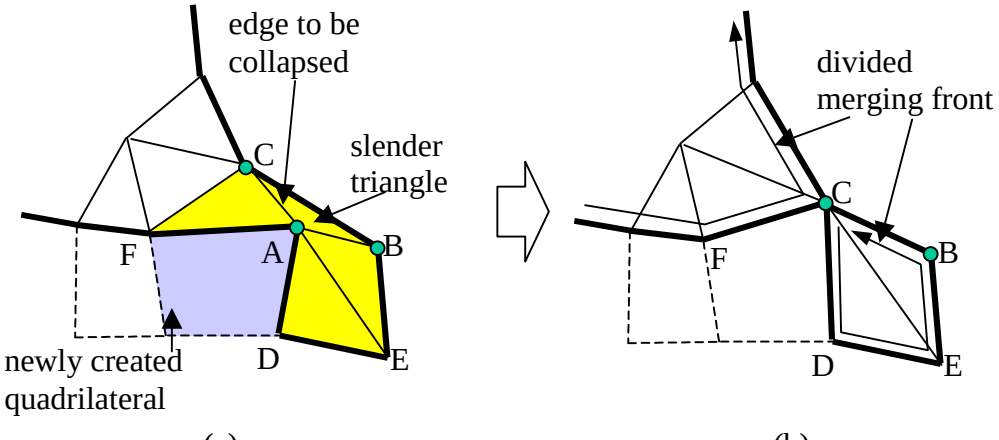

Figure 11. Merging front division: (a) detection of slender element; (b) division of merging front.

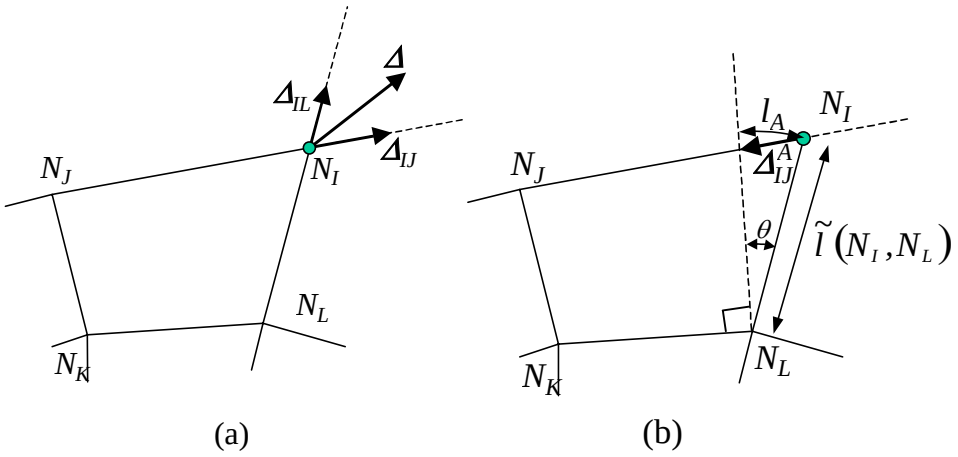

(a) (b)

Figure 12. Smoothing of floating node with one adjacent quadrilateral element: (a) decomposition of adjustment; (b) angular adjustment.

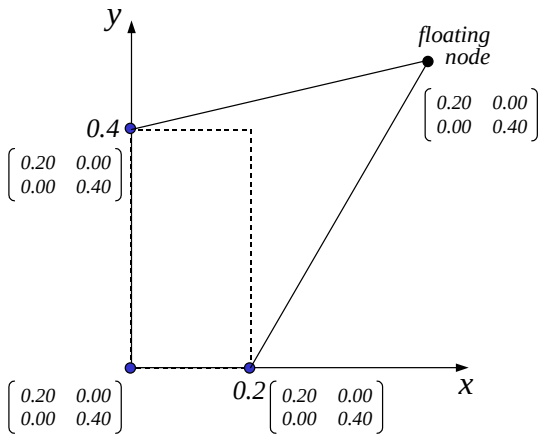

(a)

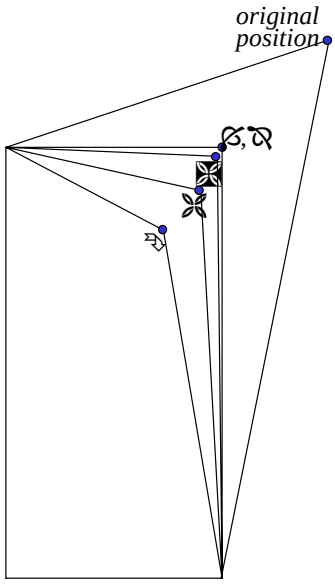

Original	(*0.3000, 0.5000*)
Iteration 1	(*0.1447, 0.3239*)
Iteration 2	(*0.1800, 0.3598*)
Iteration 3	(*0.1964, 0.3928*)
Iteration 4	(*0.2000, 0.3998*)
Iteration 5	(*0.2000, 0.4000*)

(b)

Figure 13. Numerical experiment of floating node smoothing: (a) configuration of test mesh; (b) intermediate nodal positions during iterative smoothing.

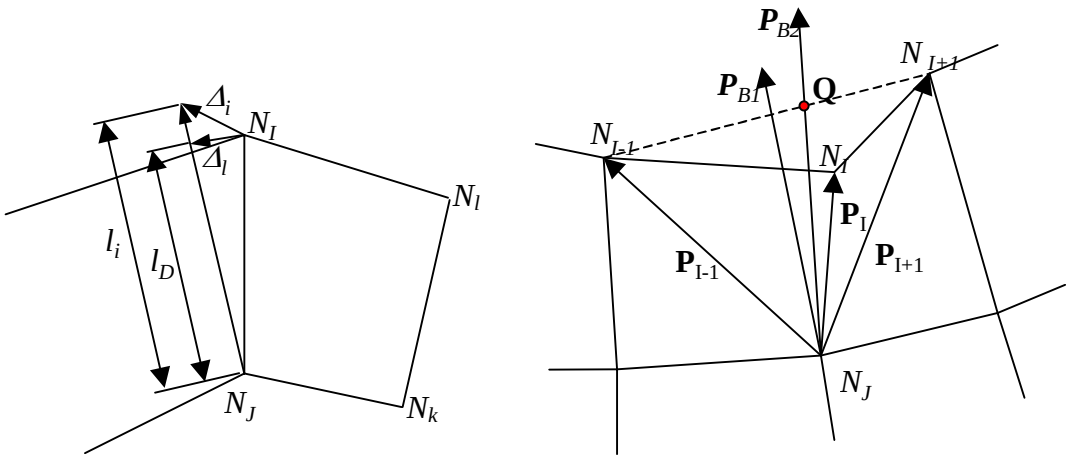

(a) (b)

Figure 14. Row node smoothing: (a) length adjustment; (b) angular adjustment.

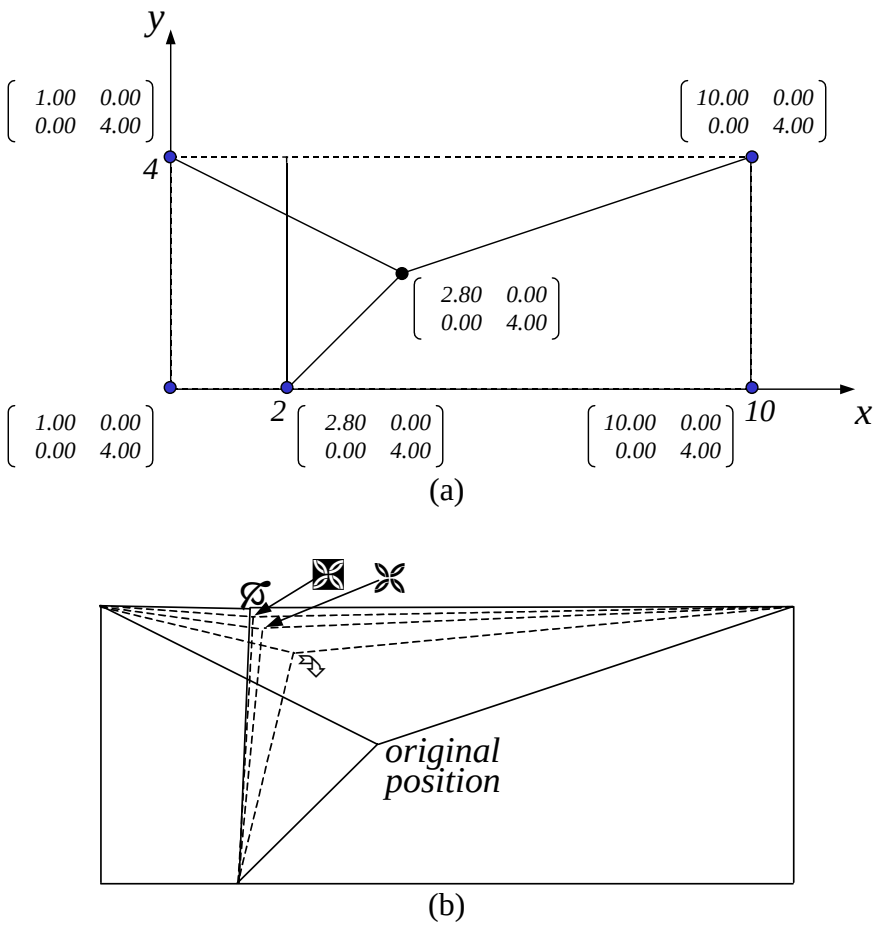

(a)

(b)

Figure 15. Numerical experiment of row node smoothing: (a) configuration of test mesh; (b) intermediate nodal positions during iterative smoothing.

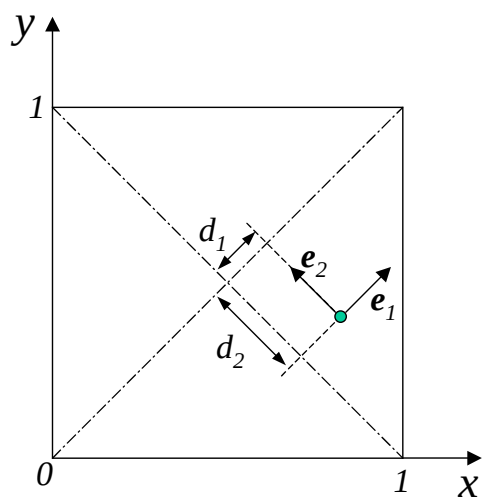

(a)

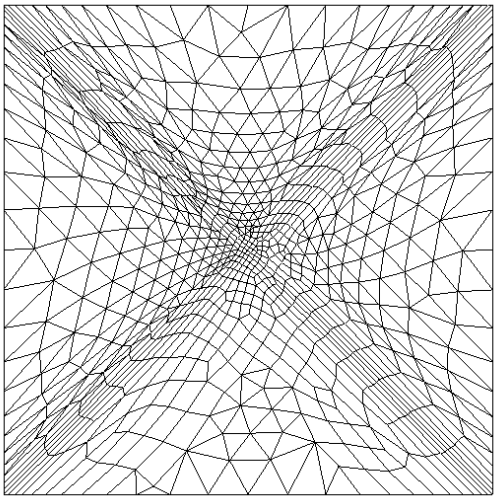

(d)

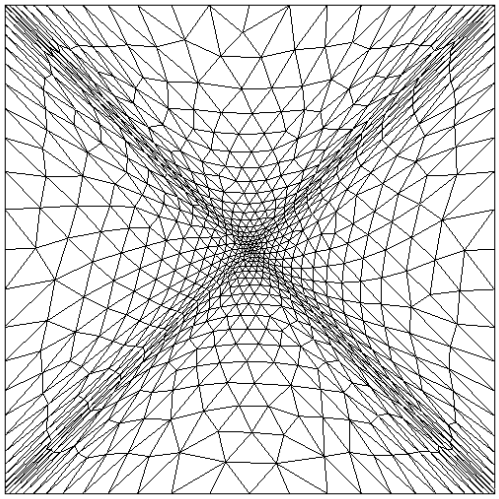

(b)

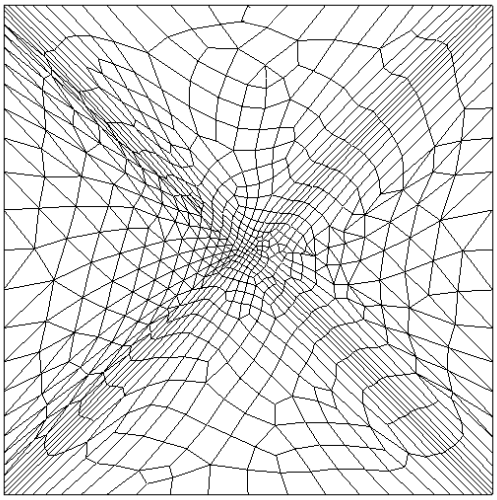

(e)

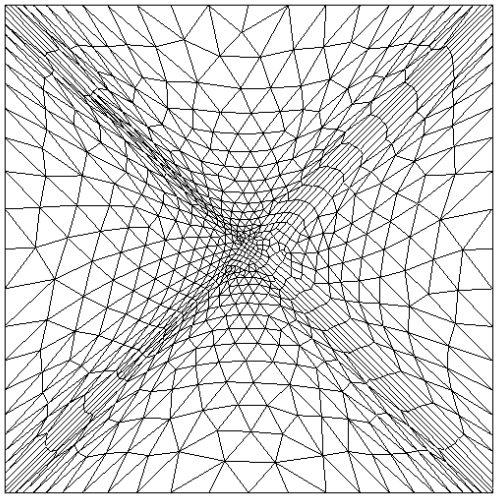

(c)

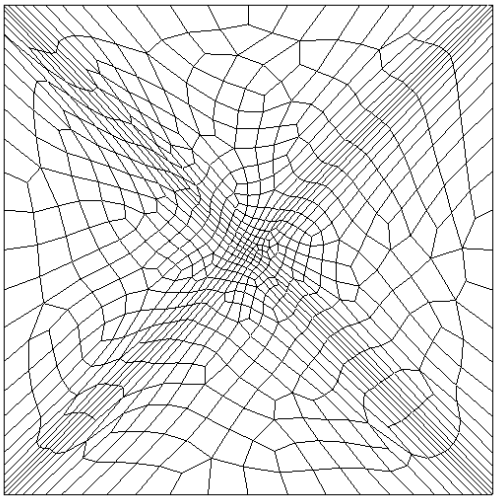

(f)

Figure 16. Example one: (a) geometry and metric specifications; (b) background triangular mesh; (c) intermediate mesh with NQ = 200; (d) intermediate mesh with NQ = 400; (e) intermediate mesh with NQ = 600; (f) final mesh with NQ = 791.

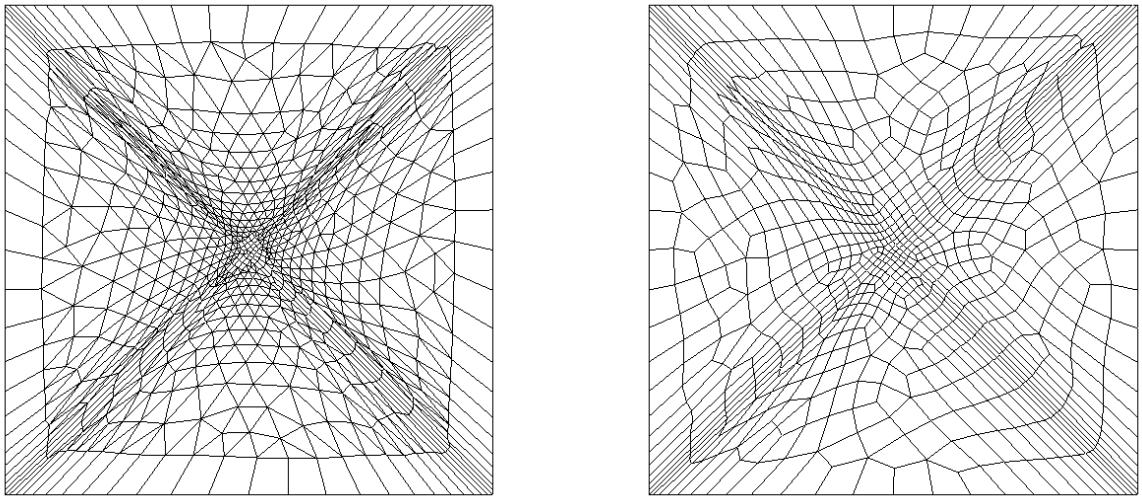

(a) (b)

Figure 17. Conversion with option of layer of boundary quadrilaterals: (a) intermediate mesh with NQ=200; (b) final mesh with NQ=768.

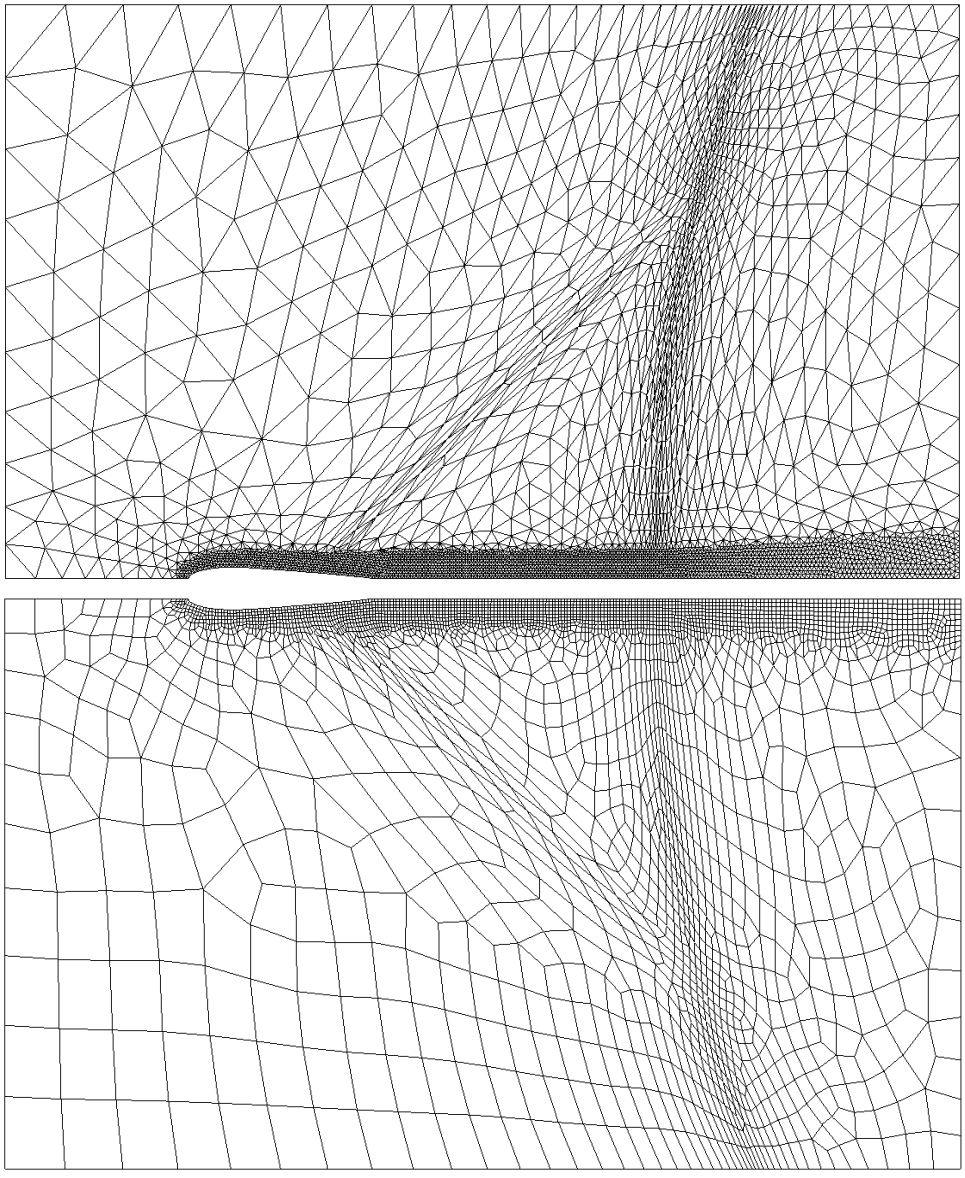

Figure 18. Example two: meshing of an airplane wing with fictitious metric specifications.

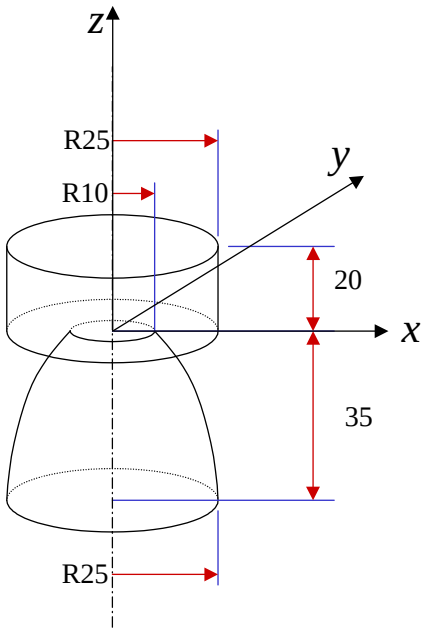

(a)

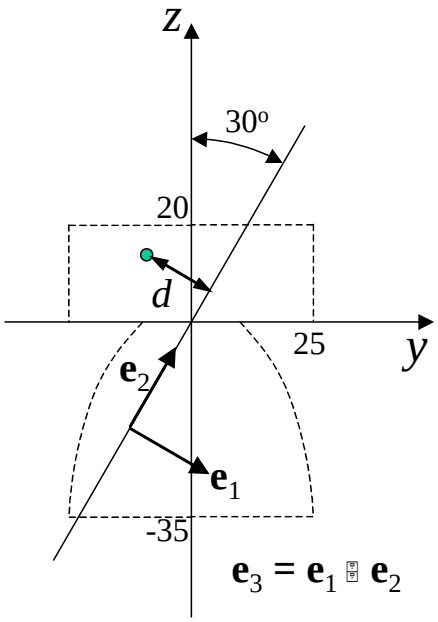

(b)

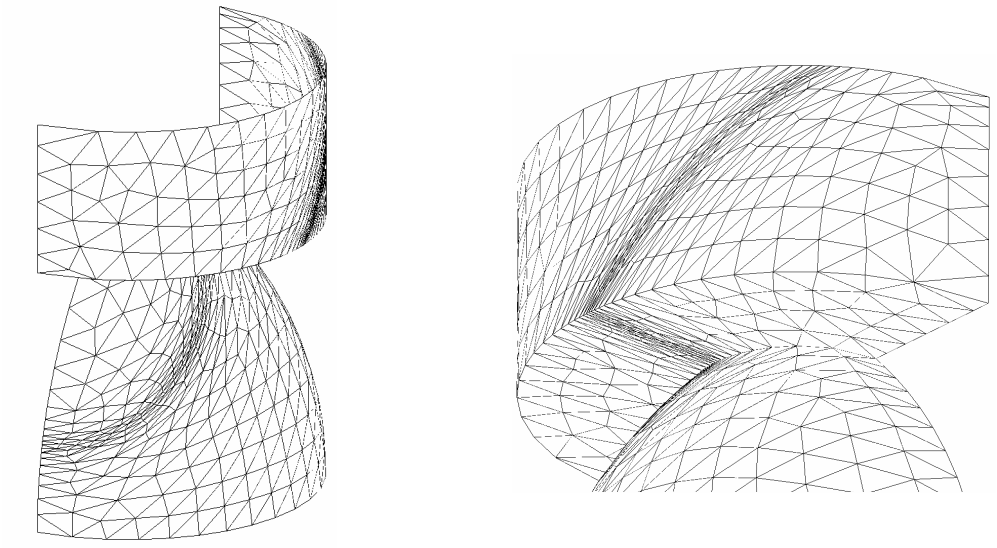

(c)

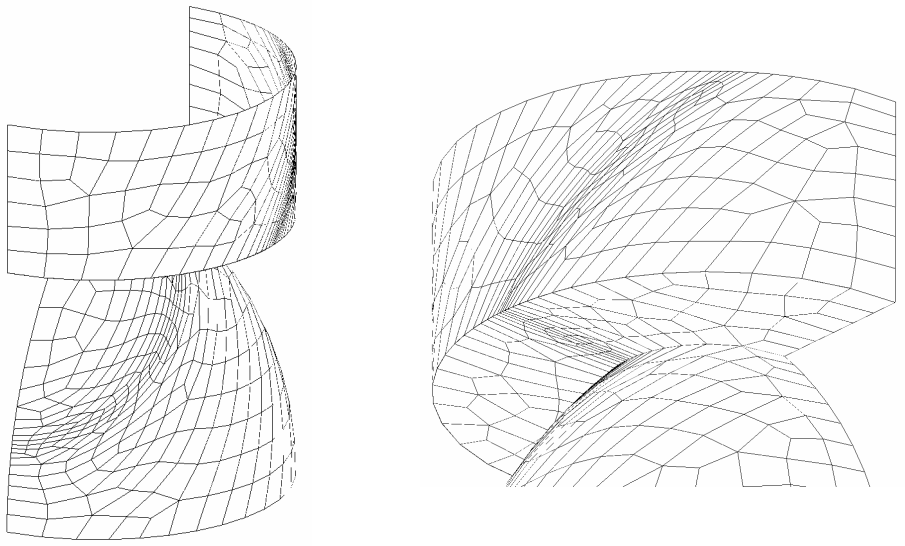

(d)

Figure 19 Example three: Meshing of a nozzle: (a) geometric definition; (b) metric tensor definition; (c) background triangular mesh; (d) converted quadrilateral mesh.

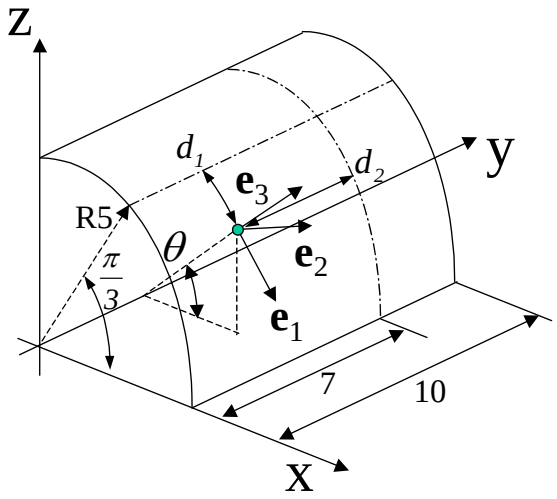

$$h_1 = c\left(2.1 - 2e^{-0.5d_1}\right)$$
$$h_2 = c\left(2.1 - 2e^{-0.5d_2}\right)$$
$$h_3 = 1$$
$$\text{where } d_1 = R\left(\theta - \frac{\pi}{3}\right),$$
$$d_2 = |y - 7|$$

Figure 20. Geometrical and metric tensor definitions for Example four.

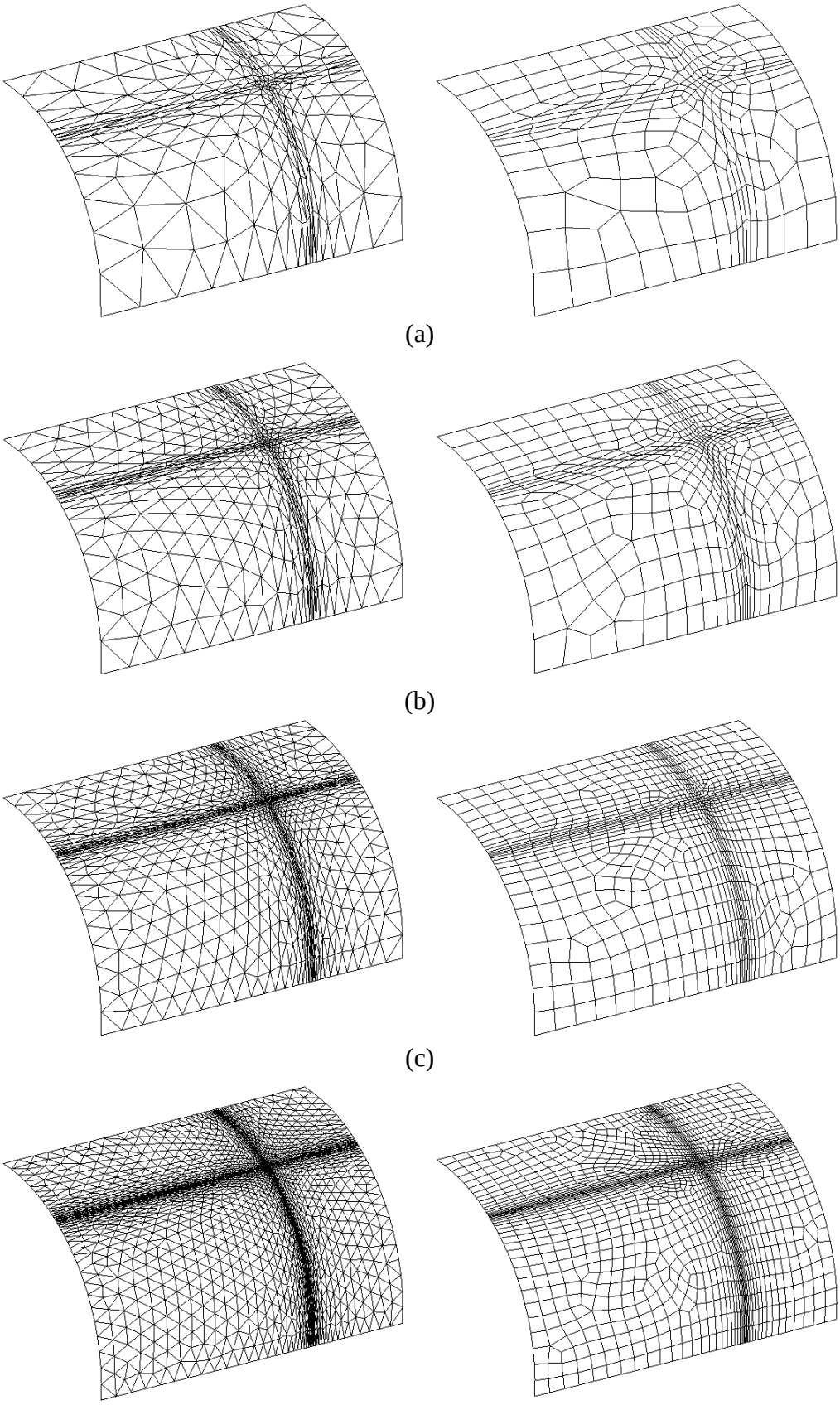

Figure 21. Background and quadrilateral meshes for Example four with various scale factors: (a) c=0.70; (b) c=0.55; (c) c=0.35, (d) c=0.18.

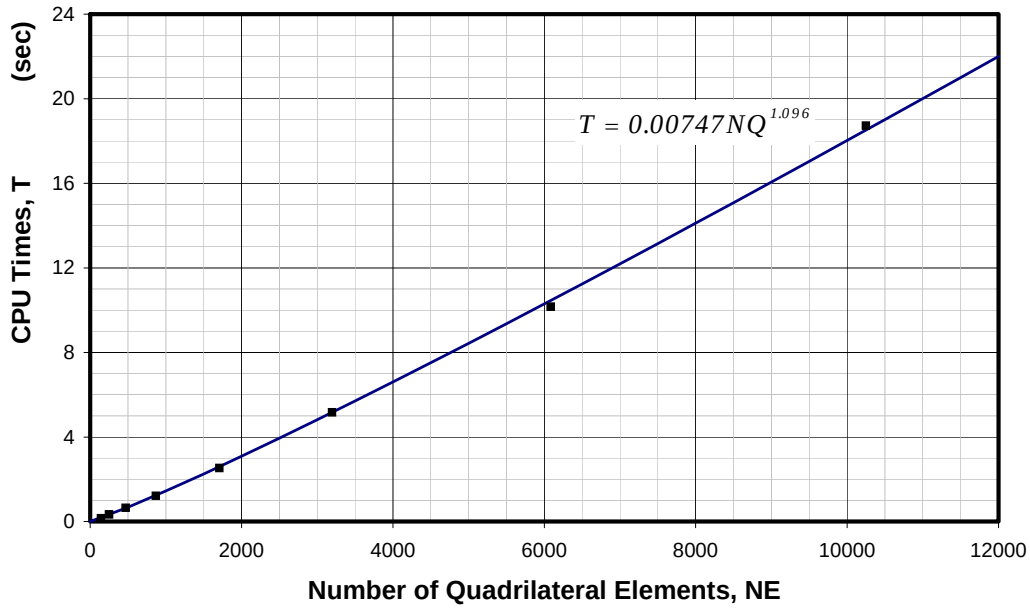

Figure 22. CPU time for quadrilateral conversion for Example four.

Table 1. Characteristics of meshes generated for Example four

Size factor *c*	Background triangular mesh		Final quadrilateral mesh		CPU time used (second)
	NN	NT	NN	NQ	
1.00	120	188	164	143	0.16
0.70	249	426	279	248	0.34
0.55	454	816	510	469	0.65
0.35	904	1684	924	867	1.22
0.25	1804	3380	1789	1708	2.53
0.18	3364	6496	3307	3196	5.16
0.13	6335	12354	6239	6086	10.16
0.10	10529	20654	10446	10249	18.72

NN= Number of nodes generated.
NT= Number of triangles generated.
NQ= Number of quadrilaterals generated.

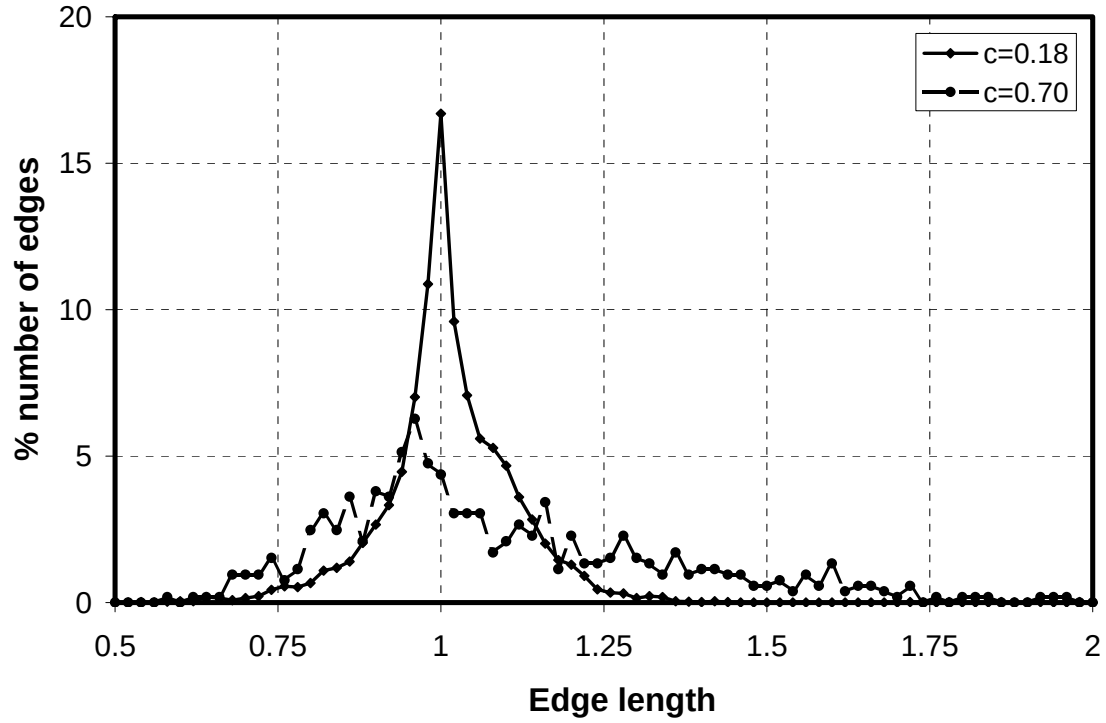

(a)

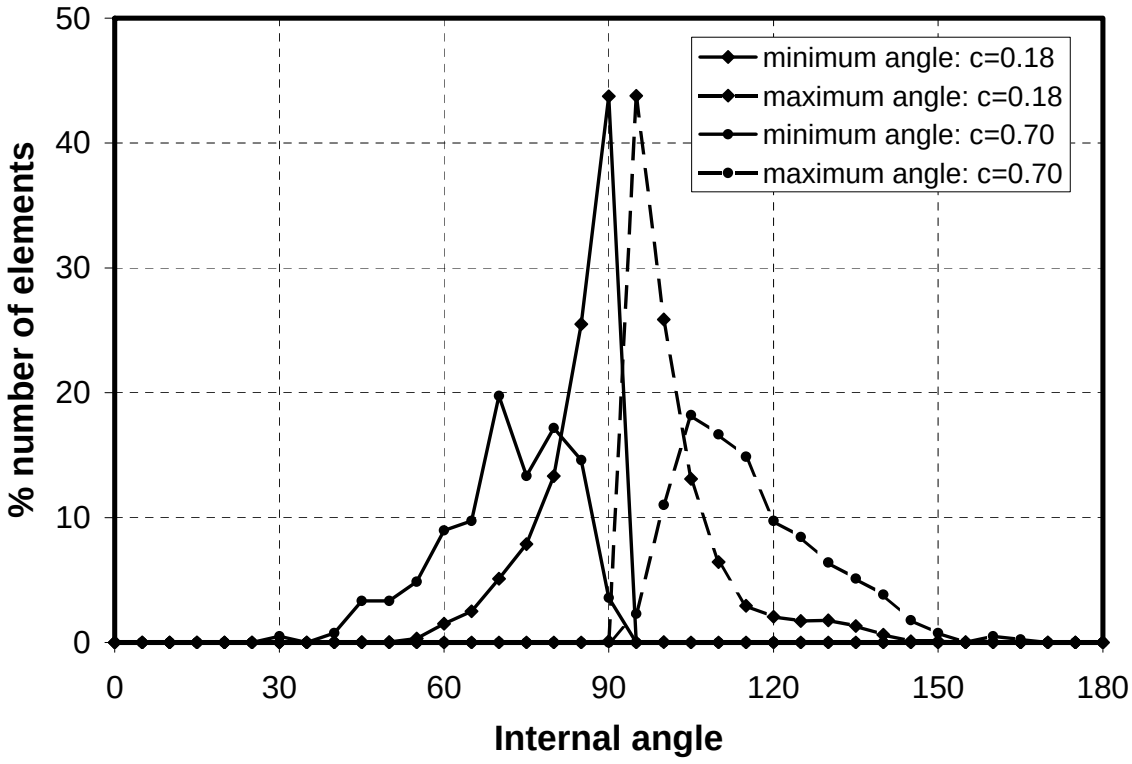

(b)

Figure 23. Anisotropic properties of quadrilateral meshes generated in Example four:
(a) distributions of metric length of edges;
(b) distributions of minimum and maximum metric angles of elements